WPJET1-CPR(17) 18221

R Dumont et al.

Scenario development for the observation of alpha-driven instabilities in JET DT plasmas

Preprint of Paper to be submitted for publication in Proceeding of 15th IAEA Technical Meeting on Energetic Particles in Magnetic Confinement Systems

This work has been carried out within the framework of the EUROfusion Consortium and has received funding from the Euratom research and training programme 2014-2018 under grant agreement No 633053. The views and opinions expressed herein do not necessarily reflect those of the European Commission.

Scenario development for the observation of alpha-driven instabilities in JET DT plasmas

R. Dumont[1], J. Mailloux[2], V. Aslanyan[3], M. Baruzzo[4], C. D. Challis[2], I. Coffey[5], A. Czarnecka[6], E. Delabie[7], J. Eriksson[8], J. Faustin[9], J. Ferreira[10], M. Fitzgerald[2], J. Garcia[1], L. Giacomelli[11], C. Giroud[2], N. Hawkes[2], Ph. Jacquet[2], E. Joffrin[1], T. Johnson[12], D. Keeling[2], D. King[2], V. Kiptily[2], B. Lomanowski[13], E. Lerche[14], M. Mantsinen[15,16], L. Meneses[10], S. Menmuir[2], K. McClements[2], S. Moradi[2], F. Nabais[10], M. Nocente[11], A. Patel[2], H. Patten[9], P. Puglia[9], R. Scannell[2], S. Sharapov[2], E. R. Solano[17], M. Tsalas[18,19], P. Vallejos[12], H. Weisen[9] and JET contributors‡.

[1]CEA, IRFM, F-13108 Saint-Paul-lez-Durance, France. [2]CCFE, Culham Science Centre, Abingdon, OX14 3DB, UK. [3]MIT PSFC, 175 Albany Street, Cambridge, MA 02039, USA. [4]Consorzio RFX, corso Stati Uniti 4, 35127 Padova, Italy. [5]Dept of Pure and Applied Physics, Queens University, Belfast, BT7 1NN, UK. [6]Institute of Plasma Physics and Laser Microfusion, 00-908 Warsaw, Hery Street 23, Poland. [7]Oak Ridge National Laboratory, Oak Ridge, Tennessee, US. [8]Dept of Physics and Astronomy, Uppsala Uni., SE-75119 Uppsala, Sweden. [9]École Polytechnique Fédérale de Lausanne (EPFL), Swiss Plasma Center (SPC), CH-1015 Lausanne, Switzerland. [10]Instituto de Plasmas e Fusão Nuclear, IST, Universidade de Lisboa, Portugal. [11]Uni. Milano-Bicocca, piazza della Scienza 3, 19126 Milano, Italy. [12]Fusion Plasma Physics, EES, KTH, SE-10044 Stockholm, Sweden. [13]Aalto Uni., P.O.Box 14100, FIN-00076 Aalto, Finland. [14]LPP-ERM/KMS, Ass. EUROFUSION-Belgian State, TEC partner, Brussels, Belgium. [15]Barcelona Supercomputing Center, Barcelona, Spain. [16]ICREA, Barcelona, Spain. [17]Laboratorio Nacional de Fusión, CIEMAT, Madrid, Spain. [18]FOM Institute DIFFER NL-3430 BE Nieuwegein, The Netherlands. [19]ITER Organization, Route de Vinon sur Verdon, 13067 St Paul Lez Durance, France.

E-mail: `remi.dumont@cea.fr`

Abstract. Energetic ions in fusion plasmas may destabilise various instabilities. Among them, Toroidal Alfvén Eigenmodes (TAEs) can be made unstable by the alpha particles resulting from fusion reactions, and may induce a significant redistribution of fast ions causing a degradation of the plasma performance, and possibly particle losses to the first wall. In next-step devices, including ITER, the potential impact of these alpha-driven TAEs remains to be precisely quantified. It is therefore essential to prepare scenarios aimed at observing alpha-driven TAEs in a future JET DT campaign. Recent experiments have been conducted in JET deuterium plasmas with this objective

‡ See the author list of "Overview of the JET results in support to ITER" by X. Litaudon et al., Nucl. Fusion **57** 1917 101901.

in mind. The requirements for maximizing TAE drive have made it necessary to operate in a domain of parameters unexplored since the installation of the ITER-like wall. Discharges at low density, large core temperatures associated with the presence of ITBs (Internal Transport Barriers) and characterised by good energetic ion confinement have been performed. ICRH has been used in the hydrogen minority heating regime to probe the TAE stability. The consequent presence of MeV ions has resulted in the observation of TAEs in many instances. The impact of several key parameters on TAE stability could therefore be studied experimentally. Modeling taking into account NBI and ICRH fast ions shows good agreement with the measured neutron rates, and has allowed extrapolations to DT plasmas to be performed.

1. Introduction

Toroidal Alfvén Eigenmodes (TAE) are weakly damped eigenmodes (gap modes) belonging to a wide class of electromagnetic instabilities[1]. They are readily destabilised by the free energy source in the distribution function of energetic ions and as a result, TAEs have been commonly observed in magnetic fusion plasmas[2]. In typical experiments, these fast ions are usually generated by auxiliary heating methods, either Neutral Beam Injection (NBI) or Ion Cyclotron Resonance Heating (ICRH) systems. In addition to these energetic populations, future fusion reactors will operate with a deuterium-tritium (DT) mixture as fuel. The resulting fusion reaction creates helium ions with a birth energy around 3.5MeV (alpha particles), i.e. well in excess of the plasma temperature. Like other fast ions, alpha particles can destabilise TAEs.

In burning plasmas, alpha-driven TAEs (α-driven TAEs) could play a crucial role in a non-linear interaction with alphas: in a worst-case scenario, the alpha population build-up results in the destabilization of α-driven TAEs, which themselves displace the alphas to more peripheral regions. This could affect the discharge performance, and even potentially cause significant losses and subsequent large fluxes on the first wall and plasma facing components. Because of the relative scarcity of DT experiments, α-driven TAEs have not been as well studied as ICRH- or NBI-driven TAEs. Given the uncertainties related to the effects of these MHD instabilities in next-step devices including ITER[3, 4, 5, 6], it is highly desirable to document the features of α-driven TAEs as extensively as possible both from a theoretical and an experimental standpoint in ongoing fusion experiments.

In the past, significant efforts have been devoted to observe and characterise α-driven TAEs, in the two only devices capable of producing DT plasmas, the Tokamak Fusion Test Reactor (TFTR) and the Joint European Torus (JET). Despite optimistic initial predictions[7], observing α-driven TAEs in TFTR has proven quite challenging, requiring scenario fine-tuning guided by numerical simulation[8]. Eventually, however, this endeavour has resulted in the unambiguous detection of α-driven TAEs for the first time in a DT experiment[9, 10]. In JET, on the other hand, it was established that α-driven TAEs could not be destabilised in hot ion H mode plasmas as a result of

the large central bulk plasma pressure. On the other hand, numerous TAEs have been routinely observed in shear optimised discharges featuring Internal Transport Barriers (ITBs). However, the use of ICRH power to create the ITBs, even at relatively low levels of power ($\gtrsim$ 1MW), provides a TAE drive in excess to the alpha-drive, associated to significant uncertainties in its precise magnitude. As a result, no firm conclusions regarding α-driven TAEs could be drawn from past DT experiments in JET[11, 12, 13].

We report here on an effort to develop a scenario adapted to the observation of alpha-driven TAEs in a forthcoming DT campaign in JET, guided by past results in JET, TFTR and numerical calculations. In section 2, the parameters adapted to the observation of α-driven TAEs in DT discharges are identified. Observations of ITBs and consequences in terms of plasma quantities are reported in section 3. In section 4, the obtained performance in terms of neutron production in these discharges are discussed, and the precise role of ICRH is detailed. TAE stability of these pulses is examined in section 5 and extrapolations to DT plasmas is the subject of section 6.

2. Operational regime

The parameters prone to the observation of α-driven TAEs may be identified by examining the balance between the TAE drive by alphas (γ_α) and the damping by different mechanisms (γ_d), which can be put in the following simplified form[14, 15, 16]

$$\gamma \equiv \gamma_\alpha - \gamma_d = -Cq^2\beta_{T\alpha}\Big(1 - \frac{\omega_\alpha^\star}{\omega}\Big)F(v_\alpha/v_A) - \gamma_d, \tag{1}$$

with q the safety factor, $\beta_{T\alpha}$ the alpha normalised pressure, ω the mode frequency. $\omega_\alpha^\star$ is the α diamagnetic frequency, F is a function of the normalised α birth velocity (v_α), v_A is the Alfvén velocity and C is a constant.

The destabilization of TAE is only possible when the diamagnetic frequency exceeds the eigenfrequency, i.e.

$$\omega_\alpha^\star \equiv -\frac{m}{r}\frac{T_\alpha}{q_\alpha B}\frac{d\log(p_\alpha)}{dr} > \omega. \tag{2}$$

In the latter expression, m is the mode poloidal number, r is the minor radius, T_α is the alpha temperature, B is the confinement field and p_α is the alpha pressure. This condition defines a threshold in terms of the alpha pressure gradient. Furthermore, Eq. 1 clearly shows that both β_α and q should be maximised.

As discussed in Ref. [11], the large bulk plasma pressure prevents the TAEs from being driven unstable in typical fusion performance scenario, despite a large alpha drive. On the other hand, TAEs have been observed in shear-optimised discharges in DT as a result of the elevated q profile, but only in the presence of ICRH power since it was essentially employed in all these pulses. The potential presence of radiofrequency-generated energetic ions in the plasma has prevented the α-driven TAEs from being unequivocally observed and characterised. In order to alleviate this risk in a future DT campaign, no ICRH will be used before the time of interest for α-driven TAE observation, i.e. the peak performance phase of the DT discharge and the afterglow

phase. In order to maximise the alpha drive in this context, it is thus necessary to make use of the full capability of the NBI system in JET to maximise the fusion reaction yield by increasing T_i, the ion temperature, since the thermonuclear reaction rate increases rapidly with the fuel temperature. On the other hand, in order to maximise the energetic particle effects, it is desirable to operate at high electron temperature T_e, which is best achieved by operating at relatively low densities. In H-mode plasmas fuelled by NBI ions, this translates into operating at low plasma current I_p, with the constraint that the alpha particle confinement remain satisfactory.

We now turn to the mode damping, which should be sufficiently low to be overcome by the alpha-drive. For gap Alvén Eigenmodes (AEs), this total damping is a combination of radiative damping γ_{rad}, collisional electron damping $\gamma_{coll,e}$, thermal electron γ_e and ion γ_i Landau damping and damping by NBI ions (γ_D and γ_T) fulfilling the condition $v_\parallel = v_A/3$. We find that in JET, the latter mechanism is largely dominant. Calculations performed with the CASTOR-K and MISHKA codes during the last DT campaign yield $\gamma_{NBI}/\omega \equiv (\gamma_D + \gamma_T)/\omega \sim 1-2\%$ whereas the maximum alpha drive was estimated to be $\gamma_\alpha/\omega \sim 0.15\%$, in other words much lower than the damping rate[11]. In TFTR and in JET, the afterglow scheme has therefore been developed to remedy this issue. In consists of switching-off the auxiliary power abruptly, and relying on the faster decay of the fast NBI deuterons compared to the alphas to observe the α-driven TAEs in the afterglow phase[9]. The afterglow scheme lends itself to the observation of α-driven TAEs if the following condition is verified

$$\left|\gamma_{NBI} e^{-t/\tau_{NBI}} + (\gamma_D + \gamma_T) e^{-t/\tau_i} + \gamma_e\right| < \gamma_\alpha e^{-t/\tau_{sd}^{(\alpha)}}, \tag{3}$$

with τ_{NBI} (resp. τ_α) the NBI (resp. alpha) ion slowing down time. τ_i is the ion confinement time and it is assumed that electron damping remains constant during this phase. In practice, this translates into the condition $\tau_{NBI} < \tau_\alpha$, which is well verified for deuterium NBI ions.

The scenario development presented in the present paper is performed in deuterium plasmas, in which α-driven TAEs are by definition absent. In order to probe the distance to the TAE instability threshold of the obtained plasmas, ions in the MeV range of energies are created using ICRH. In all presented pulses with ICRH power, standard hydrogen minority heating has been used. The central confinement field is $B_0 = 3.4$T and the ICRH frequency is set to 51MHz, locating the fundamental resonance in the vicinity of the magnetic axis. The hydrogen concentration was in the range $\sim 2-7\%$.

Various plasma currents have been tested, in the range $I_p = 2-3$MA. It has been established that $I_p = 2.5$MA constitutes a good compromise between satisfactory energetic particle confinement (which has also been shown to hold true for 3.5MeV alpha particles in numerical simulations) and low density operation.

3. Internal Transport Barriers in JET-ILW

As discussed previously, it is desirable to produce low density plasmas in order to maximise the fast hydrogen ion slowing-down time. However, since the installation of the ITER-like Wall (ILW) in JET[17], typical plasma densities are higher than those obtained with the former carbon wall (C-wall)[18]. In the present effort, it is desirable to reconcile the contradictory requirements of elevated q-profile plasmas, which is typically achieved by switching-on the NBI power early in the discharge with the requirements of obtaining low density in the peak-performance period. In Fig. 1 is plotted the density obtained in the peak-performance phase versus the density at the NBI switch-on time. This figure was produced by selecting pulses with comparable total NBI power and $I_p \leq 2.75$MA. The error-bars come from the fact that the time of peak performance is defined as a period of 100-200ms, during which the density may vary slightly.

It is clearly observed that it is beneficial to start the plasma with as low a density as possible, while obviously still fulfilling the operational limits of the JET ILW. This was done by implementing the so-called staggered-PINI recipe, consisting of firing the various NBI injectors with various delays depending on their respective shine-through limit and selected voltage. This recipe has allowed lower densities at the time of peak performance to be achieved compared to other pulses operated in JET-ILW, as shown in Fig. 2.

In order to obtain elevated values of the safety factor q, a common method employed in advanced scenarios is to inject external power during the current ramp-up phase in order to slow-down the current profile diffusion process[19, 20]. To confirm the applicability of this method in JET-ILW, several similar shots have been performed, varying only the NBI switch-on time (t_{NBI}). The corresponding time traces are shown in Fig. 3, and the resulting q-profile at the time of NBI switch-on reconstructed using EFIT[21] constrained with polarimetry and kinetic profiles is shown in Fig. 4.

This confirms that the variation of the NBI switch-on time is an efficient method to produce high values of the central safety factor (q_0). Although EFIT predicts a very low shear in an extended region near the plasma center, it should be pointed out that it is often difficult to have a high accuracy of the equilibrium reconstruction in the central region. Nevertheless, except in a very limited number pulses in which Alfvén Cascades were observed, indicating a negative shear in the plasma center, no experimental indications of systematic q-profile reversal were obtained.

Unsurprisingly, we note that the modifications induced by varying t_{NBI} are not limited to q_0. On the bottom graph of Fig. 4, it is clearly seen that the neutron rate at the time of peak performance varies significantly from pulse to pulse. As an illustration, of these four discharges, pulse #90189 achieves $q_0 \approx 1.5$ with the highest neutron rate, whereas pulse #90194 is characterised by $q_0 \approx 2.5$, but a significantly lower neutron rate. Therefore, since both parameters are important for TAE excitation, a trade-off between q_0 and overall performance is required.

The presence of an extended central region of low positive shear is known to be

prone to the triggering of ITBs when the minimal value of q reaches rational values[22]. For the first time since the installation of the ILW, ITBs have been clearly observed in a number of discharges performed in the framework of this experimental effort. Fig. 5 shows time traces of pulses #92054 with $P_{NBI} \approx 25$MW. This pulse uses only NBI power at the peak performance time of the discharge, thus fulfilling the criteria listed above for α-driven TAE observation in DT discharges. ICRH power is applied after the time of peak performance in order to ensure a safe plasma termination.

In this discharge, it is observed that $T_i(0)$ and central toroidal rotation(ω_{tor}) steadily increase with time. The start time of the ITB development is consistent with the appearance of the $q = 2$ surface in the plasma, although the equilibrium reconstruction is is not accurate enough to reach a firm conclusion on this point. The electron temperature increases as well but at a slower rate, since NBI heating preferentially acts as an ion heating source. The resulting electron, ion and density profiles at the times shown by the dashed lines in Fig. 5 are shown in Fig. 6. These profiles have respectively been produced using data from Charge Exchange Recombination Spectroscopy (CXRS), Electron Cyclotron Emission (ECE) radiometer and High Resolution Thomson Scattering (HRTS) systems although good consistency between the various systems installed in JET has been achieved in these discharges.

The central ion temperature was found to reach $T_i(0) \gtrsim 10$keV in high power discharges, whereas $T_e(0) \sim 5$keV. As a result of the ITB appearance, the density profiles is peaked, as shown in shown in the bottom graph Fig. 6. Simultaneously, it is also observed that the $T_i(0)$ and $T_e(0)$ start to decrease slightly before the peak the end of the NBI-only phase, which is caused by the core impurity accumulation resulting from the density peaking, consistently with past observations performed in JET equipped with the C-wall[23]. The involved impurities have been identified to be mostly tungsten and nickel. It must be pointed out that this process does not compromise the objectives of the present effort from being reached, since the impurity accumulation is not severe enough at the time of peak performance to induce a termination of the considered pulse by the device protection systems.

4. Neutron rate and performance

A central goal of the present scenario development is to establish that sufficient fusion performance can be obtained in an extrapolated DT plasma to ensure that α-driven TAEs can be observed, despite the requirement that no ICRH power must be used before the time of peak performance. In Fig. 7 is plotted the neutron rate at peak performance versus the total injected power, including in NBI and NBI+ICRH phases for all successful pulses. ICRH can contribute to the neutron rate through 1) an increase of global plasma quantities (electron and ion temperature, essentially) on the one hand, 2) the generation of energetic deuterons by harmonic heating[24]. Calculations performed with the CYRANO[25] and EVE[26] codes for various pulses in which ICRH power was used up to 4.5MW with hydrogen concentrations $n_H/n_e \sim 2 - 7\%$, second harmonic

deuterium damping never exceeds 25% of the total RF power damping. Although Neutral Particle Analyzers (NPAs) do observe non-thermal deuterium ions in some pulses, the resulting deuterium acceleration appears to be insufficient to significantly contribute to the neutron rate. This is further confirmed by neutron spectroscopy analysis of these pulses[27], which shows that the RF contribution to the neutron rate does not exceed 15% even at low levels of hydrogen concentrations ($\lesssim 2\%$).

In Fig. 8 is plotted the measured neutron rate versus $n_D P_{NBI} \tau_{s,e}$ with n_D the deuterium density (deduced from the electron density and Z_{eff} measurement), and $\tau_{s,e}$ the electron slowing-down time. The beam-target reaction rate computed with the PENCIL code using the measured kinetic profiles is found to scale linearly with this quantity, as it should[28], and to agree well with the experimental measurement for low to medium NBI power. It is observed that at high NBI power, significant departure occurs, which results from the thermonuclear contribution to the neutron rate.

In order to further characterise the role of ICRH power, pulses #92415 and #92416 have been performed at 2.5MA, and the afterglow scheme has been tested for an operational standpoint in both. As shown in Fig. 9, both shots are identical except for the fact that ICRH was only used for shot termination in #92415, whereas it was applied throughout in pulse #92416, resulting in a significant increase of the neutron rate in the latter with respect to the former. This is caused by a combination of higher ion temperature and density in the second case.

The TRANSP code[29] has been used to interpret the experimental measurement of pulse #92416, and estimate the various contributions to the total neutron rate. The result is shown in Fig. 10. The ITB development is found to result in a significant increase of the thermonuclear contribution to the neutron rate. The benefit from this large contribution is that when the afterglow phase starts, the associated neutron rate decay occurs on the energy confinement timescale, whereas the beam-target contribution decrease is linked to the slowing-down time of NBI ions. In a DT discharge, this means that the alpha production remains substantial during a finite time following the power switch-off. The alpha decay, resulting from the combination of decreasing ion temperature and density and 3.5MeV alpha slowing-down, is therefore expected to occur on a timescale significantly longer compared to the NBI ion slowing-down time.

As shown in Fig. 8, in pulses performed with 25MW of NBI power and using only NBI power before peak performance, it is found that up to 50% of the neutron rate comes for the thermal fusion reactions.

5. TAE stability in deuterium plasmas

The objective of ICRH power use in these deuterium pulses is to probe some of the best performing discharges with respect to TAE stability. This is what is done in the comparison between pulses #92415 and #92416 (Fig. 9). In pulse #92415, no significant AE activity has been recorded by the Mirnov coils. In most discharges with RF power $P_{RF} \gtrsim 2$MW, on the other hand, TAEs are observed in the range 100-200kHz. As shown

in Fig. 11, this is the case in pulse #92416 with ICRH power throughout.

In this discharge, it is observed that TAEs are present until $t \approx 5.3$s. At this time, the NBI power is increased from 10MW to 25MW. The TAE frequency shifts upwards as a result of the toroidal velocity increase. At $t \approx 5.5$s, it starts to shift downwards following the decrease of $v_A \propto 1/n_e^{1/2}$ caused by the density increase caused by the NBI fuelling. At $t \approx 5.6$s, the TAEs disappear consistently with the damping by NBI ions despite the presence of 5MW of ICRH power. The afterglow phase starts at $t = 6.1$s and is following by the reappearance of the TAEs with a delay ~ 100ms, which is consistent with the deuterium ion slowing-down.

Fig. 12 shows a zoom on the TAEs reappearing at $t \approx 6.2$s. The toroidal array of Mirnov coils installed on JET allows the toroidal mode numbers (n) to be estimated. It shows that the corresponding TAEs are characterised by $n = 4, 5$ and 6. Also visible on this figure is the signal from the active antenna used for TAE excitation in JET[30]. Although this system has also been used in these discharges, the obtained results will be reported in a separate article.

In order to further characterise these modes, the HELENA[31] and MISHKA[32] have been run using the data from EFIT at $t = 6.2$s as input. The result from the MISHKA calculation corresponding to the mode $n = 5$ is displayed in Fig. 13. It shows a TAE located at normalised radius $\rho \approx 0.4$ dominated by poloidal components $m = 10$ and $m = 11$. It is consistent with experimental data, although the MHD diagnostics in JET do not allow a precise radial localization of the modes to be performed. Nevertheless, reflectometry data does not indicate the presence of any TAEs in the outer parts of the plasma at this time of the discharge, which is consistent with the presence of a core-localised TAE.

Finally, it must be noted that the linear MHD calculations performed with MISHKA display a large sensitivity with respect to the precise value of q_0, as a result of the very low shear predicted by EFIT. Experimentally, however, TAEs are commonly observed in discharges with ICRH power, and appear to be quite robust with respect to changes in the plasma parameters, including q. This could be an indication of the fact that the q-profile is not as flat as predicted. Non-linear MHD calculations, including sensitivity studies, in the presence of energetic hydrogen ions retaining finite orbit effects performed with the SELFO[33] and VENUS[34] codes are ongoing and will be the subject of a future publication.

6. Extrapolation to deuterium-tritium discharges

In order to establish the relevance of the developed scenario in terms of α-driven TAE observation, it is necessary to perform extrapolations of the performed deuterium pulses to a DT mixture. This has been done performing several runs with the TRANSP code. The reference pulse used for these calculations is #92054, using NBI only in its peak performance phase, and already presented in section 3. The first step is to carefully interpret the measurements by using the experimental values of T_i, T_e, n_e and ω_{tor}. The

measured effective charge (Z_{eff}) was used as well assuming the Z_{eff} profile was flat. At this stage, the main source of uncertainty corresponds to the impurity content of the discharge. Several hypotheses have been tested in this domain, with the objective of reproducing the plasma energy W_p, neutron rate R_{nt} and radiated power P_{rad}:

(i) When the only impurity is assumed to be W and T_i is taken to be the experimental value, W_p is correctly reproduced. On the other hand, both R_{nt} and P_{rad} are overestimated.

(ii) When the only impurity is assumed to be beryllium (Be), W_p is well recovered, but R_{nt} is significantly underestimated as Z_{eff} increases, pointing to an excessive dilution with respect to the experiment. P_{rad} is much too low compared to experimental bolometry measurements.

(iii) When the only impurity is assumed to be W but T_i is chosen to be the lower range of error bars of CXRS measurements, it is possible to reproduce W_p and P_{rad} with good accuracy. R_{nt} is also correctly recovered, with only a slight underestimation at the time of peak performance.

These results are summarised in Fig. 14. The outcome of these simulations is that the actual plasma probably contains a mix of W and Be (as well as other light impurities). Given the uncertainties in this domain, the DT extrapolation has been performed by assuming that W was the only impurity, but that T_i had a finite range of uncertainty corresponding to options 1 and 3 above.

This pulse has been used as a basis for extrapolation, replacing both fuel and NBI deuterium ions by a 50%-50% mixture of deuterium and tritium. This has allowed the expected alpha density, pressure and corresponding $\beta_{T\alpha}$ to be estimated. The obtained result is shown in Fig. 15. As discussed previously, the finite range of T_i provides a range of $\beta_{T\alpha}$ values. It turns out that the obtained $\beta_{T\alpha}$ is comparable, or even slightly larger, than what was achieved in successful TFTR experiments[9]. Although this extrapolation can not replace comprehensive simulations taking into account all scenario, energetic particles and MHD aspects, it constitutes an encouragement to pursue the engaged efforts in view of future DT campaigns in JET.

7. Conclusions

A significant effort has been engaged in view of preparing for the observation of α-driven TAEs in the upcoming DT campaign of JET. In this perspective, deuterium discharges have been performed at comparatively low densities, elevated q-profiles and using only NBI power prior to the peak performance phase of the pulse. The plasma current has been chosen $I_p = 2.5$MA, which has been found to constitute a good compromise between low density operation and good energetic particle confinement. The magnetic field $B_T = 3.4$T allows ICRH to be used for TAE probing purposes by locating the fundamental hydrogen cyclotron layer close to the magnetic axis by generating a significant population of energetic hydrogen ions. With these parameters,

ITBs have been unambiguously observed for the first time since the installation of the ILW in JET. They have allowed the central ion temperature to reach $T_i \gtrsim 13$keV with 25MW of NBI power, resulting in a neutron rate $R_{NT} \gtrsim 1.2 \times 10^{16}/s$, with a contribution of the thermal neutron production up to $\sim 50\%$. By using ICRH, TAEs have been routinely observed in the range 100-200kHz when $P_{ICRH} \gtrsim 1 - 2$MW. They have been observed to be damped at high NBI power. Linear MHD calculations and the absence of any edge TAE on reflectometry measurements for these discharges show that these modes are core-localised. Interpretative integrated simulations of the best performing discharges have been performed using various hypotheses in terms of impurity content, and then extrapolated to DT plasmas. They predict that normalised alpha pressure values could be comparable or even slightly larger than values measured in successful α-driven TAE experiments in TFTR. It is planned to confirm the obtained results by performing discharges at higher NBI power in an upcoming deuterium campaign, and also consolidate extrapolations to DT by performing similar pulses in pure tritium plasmas before applying this scenario to the next JET DT campaign.

Acknowledgments

This work has been carried out within the framework of the EUROfusion Consortium and has received funding from the Euratom research and training programme 2014-2018 under grant agreement No 633053. The views and opinions expressed herein do not necessarily reflect those of the European Commission.

References

[1] C. Z. Cheng and M. S. Chance. Low-n shear alfvén spectra in axisymmetric toroidal plasmas. *The Physics of Fluids*, 29(11):3695–3701, 1986.

[2] King-Lap Wong. A review of alfvén eigenmode observations in toroidal plasmas. *Plasma Physics and Controlled Fusion*, 41(1):R1, 1999.

[3] N.N. Gorelenkov, S.D. Pinches, and K. Toi. Energetic particle physics in fusion research in preparation for burning plasma experiments. *Nuclear Fusion*, 54(12):125001, 2014.

[4] S. D. Pinches, I. T. Chapman, Ph. W. Lauber, H. J. C. Oliver, S. E. Sharapov, K. Shinohara, and K. Tani. Energetic ions in iter plasmas. *Physics of Plasmas*, 22(2):021807, 2015.

[5] M Schneller, Ph Lauber, and S Briguglio. Nonlinear energetic particle transport in the presence of multiple alfvnic waves in iter. *Plasma Physics and Controlled Fusion*, 58(1):014019, 2016.

[6] M. Fitzgerald, S.E. Sharapov, P. Rodrigues, and D. Borba. Predictive nonlinear studies of tae-induced alpha-particle transport in the q =10 iter baseline scenario. *Nuclear Fusion*, 56(11):112010, 2016.

[7] R.V. Budny, M.G. Bell, H. Biglari, M. Bitter, C.E. Bush, C.Z. Cheng, E.D. Fredrickson, B. Grek, K.W. Hill, H. Hsuan, A.C. Janos, D.L. Jassby, D.W. Johnson, L.C. Johnson, B. LeBlanc, D.C. McCune, D.R. Mikkelsen, H.K.Park, A.T. Ramsey, S.A. Sabbagh, S.D. Scott, J.F. Schivell, J.D. Strachan, B.C. Stratton, E.J. Synakowski, G. Taylor, M.C. Zarnstorff, and S.J. Zweben. Simulations of deuterium-tritium experiments in tftr. *Nuclear Fusion*, 32(3):429, 1992.

[8] D.A. Spong, C.L. Hedrick, and B.A. Carreras. Strategies for modifying alpha driven tae thresholds through q profile and ion temperature control. *Nuclear Fusion*, 35(12):1687, 1995.

[9] R. Nazikian, G. Y. Fu, S. H. Batha, M. G. Bell, R. E. Bell, R. V. Budny, C. E. Bush, Z. Chang,

Y. Chen, C. Z. Cheng, D. S. Darrow, P. C. Efthimion, E. D. Fredrickson, N. N. Gorelenkov, B. Leblanc, F. M. Levinton, R. Majeski, E. Mazzucato, S. S. Medley, H. K. Park, M. P. Petrov, D. A. Spong, J. D. Strachan, E. J. Synakowski, G. Taylor, S. Von Goeler, R. B. White, K. L. Wong, and S. J. Zweben. Alpha-particle-driven toroidal alfvén eigenmodes in the tokamak fusion test reactor. *Phys. Rev. Lett.*, 78:2976–2979, Apr 1997.

[10] S.J. Zweben, R.V. Budny, D.S. Darrow, S.S. Medley, R. Nazikian, B.C. Stratton, E.J. Synakowski, and G. Taylor for the TFTR Group. Alpha particle physics experiments in the tokamak fusion test reactor. *Nuclear Fusion*, 40(1):91, 2000.

[11] S.E. Sharapov, D. Borba, A. Fasoli, W. Kerner, L.-G. Eriksson, R.F. Heeter, G.T.A. Huysmans, and M.J. Mantsinen. Stability of alpha particle driven alfvén eigenmodes in high performance jet dt plasmas. *Nuclear Fusion*, 39(3):373, 1999.

[12] S.E. Sharapov, B. Alper, D. Borba, L.-G. Eriksson, A. Fasoli, R.D. Gill, A. Gondhalekar, C. Gormezano, R.F. Heeter, G.T.A. Huysmans, J. Jacquinot, A.A. Korotkov, P. Lamalle, M.J. Mantsinen, D.C. McDonald, F.G. Rimini, D.F.H. Start, D. Testa, P.R. Thomas, and JET Team. Energetic particle physics in jet. *Nuclear Fusion*, 40(7):1363, 2000.

[13] S. E. Sharapov, L.-G. Eriksson, A. Fasoli, G. Gorini, J. Kllne, V. G. Kiptily, A. A. Korotkov, A. Murari, S. D. Pinches, D. S. Testa, and P. R. Thomas. Chapter 5: Burning plasma studies at jet. *Fusion Science and Technology*, 53(4):989–1022, 2008.

[14] G. Y. Fu and J. W. Van Dam. Excitation of the toroidicityinduced shear alfvén eigenmode by fusion alpha particles in an ignited tokamak. *Physics of Fluids B: Plasma Physics*, 1(10):1949–1952, 1989.

[15] C. Z. Cheng. Alpha particle destabilization of the toroidicityinduced alfvén eigenmodes. *Physics of Fluids B: Plasma Physics*, 3(9):2463–2471, 1991.

[16] B N Breizman and S E Sharapov. Energetic particle drive for toroidicity-induced alfven eigenmodes and kinetic toroidicity-induced alfven eigenmodes in a low-shear tokamak. *Plasma Physics and Controlled Fusion*, 37(10):1057, 1995.

[17] F. Romanelli and JET EFDA Contributors. Overview of the jet results with the iter-like wall. *Nuclear Fusion*, 53(10):104002, 2013.

[18] E. Joffrin, M. Baruzzo, M. Beurskens, C. Bourdelle, S. Brezinsek, J. Bucalossi, P. Buratti, G. Calabro, C.D. Challis, M. Clever, J. Coenen, E. Delabie, R. Dux, P. Lomas, E. de la Luna, P. de Vries, J. Flanagan, L. Frassinetti, D. Frigione, C. Giroud, M. Groth, N. Hawkes, J. Hobirk, M. Lehnen, G. Maddison, J. Mailloux, C.F. Maggi, G. Matthews, M. Mayoral, A. Meigs, R. Neu, I. Nunes, T. Puetterich, F. Rimini, M. Sertoli, B. Sieglin, A.C.C. Sips, G. van Rooij, I. Voitsekhovitch, and JET-EFDA Contributors. First scenario development with the jet new iter-like wall. *Nuclear Fusion*, 54(1):013011, 2014.

[19] C D Challis, Yu F Baranov, G D Conway, C Gormezano, C W Gowers, N C Hawkes, T C Hender, E Joffrin, J Mailloux, D Mazon, S Podda, R Prentice, F G Rimini, S E Sharapov, A C C Sips, B C Stratton, D Testa, and K-D Zastrow. Effect of q-profile modification by lhcd on internal transport barriers effect of q-profile modification by lhcd on internal transport barriers in jet. *Plasma Physics and Controlled Fusion*, 43(7):861, 2001.

[20] C. Gormezano, C. D. Challis, E. Joffrin, X. Litaudon, and A. C. C. Sips. Chapter 4: Advanced tokamak scenario development at jet. *Fusion Science and Technology*, 53(4):958–988, 2008.

[21] D.P. O'Brien, L.L. Lao, E.R. Solano, M. Garribba, T.S. Taylor, J.G. Cordey, and J.J. Ellis. Equilibrium analysis of iron core tokamaks using a full domain method. *Nuclear Fusion*, 32(8):1351, 1992.

[22] E. Joffrin, C.D. Challis, G.D. Conway, X. Garbet, A. Gude, S. Günter, N.C. Hawkes, T.C. Hender, D.F. Howell, G.T.A. Huysmans, E. Lazzaro, P. Maget, M. Marachek, A.G. Peeters, S.D. Pinches, S.E. Sharapov, and JET-EFDA contributors. Internal transport barrier triggering by rational magnetic flux surfaces in tokamaks. *Nuclear Fusion*, 43(10):1167, 2003.

[23] R. Dux, C. Giroud, K.-D. Zastrow, and JET EFDA contributors. Impurity transport in internal transport barrier discharges on jet. *Nuclear Fusion*, 44(2):260, 2004.

[24] M. Schneider, T. Johnson, R. Dumont, J. Eriksson, L.-G. Eriksson, L. Giacomelli, J.-B. Girardo, T. Hellsten, E. Khilkevitch, V.G. Kiptily, T. Koskela, M. Mantsinen, M. Nocente, M. Salewski, S. E. Sharapov, A. E. Shevelev, and JET Contributors. Modelling third harmonic ion cyclotron acceleration of deuterium beams for jet fusion product studies experiments. *Nuclear Fusion*, 56(11):112022, 2016.

[25] E Lerche, D Van Eester, A Krasilnikov, J Ongena, P Lamalle, and JET-EFDA contributors. Modelling of d majority icrh at jet: impact of absorption at the doppler-shifted resonance. *Plasma Physics and Controlled Fusion*, 51(4):044006, 2009.

[26] R. J. Dumont and D. Zarzoso. Heating and current drive by ion cyclotron waves in the activated phase of iter. *Nuclear Fusion*, 53(1):013002, 2013.

[27] M. Gatu Johnson, L. Giacomelli, A. Hjalmarsson, M. Weiszflog, E. Andersson Sundén, S. Conroy, G. Ericsson, C. Hellesen, J. Källne, E. Ronchi, H. Sjöstrand, G. Gorini, M. Tardocchi, A. Murari, S. Popovichev, J. Sousa, R. C. Pereira, A. Combo, N. Cruz, and JET EFDA Contributors. The tofor neutron spectrometer and its first use at jet. *Review of Scientific Instruments*, 77(10):10E702, 2006.

[28] J.D. Strachan, M.G. Bell, M. Bitter, R.V. Budny, R.J. Hawryluk, K.W. Hill, H. Hsuan, D.L. Jassby, L.C. Johnson, B. LeBlanc, D.K. Mansfield, E.S. Marmar, D.M. Meade, D.R. Mikkelsen, D. Mueller, H.K. Park, A.T. Ramsey, S.D. Scott, J.A. Snipes, E.J. Synakowski, G. Taylor, and J.L. Terry. Neutron emission from tftr supershots. *Nuclear Fusion*, 33(7):991, 1993.

[29] R.J Goldston, D.C McCune, H.H Towner, S.L Davis, R.J Hawryluk, and G.L Schmidt. New techniques for calculating heat and particle source rates due to neutral beam injection in axisymmetric tokamaks. *Journal of Computational Physics*, 43(1):61 – 78, 1981.

[30] P. Puglia, W. Pires de Sa, P. Blanchard, S. Dorling, S. Dowson, A. Fasoli, J. Figueiredo, R. Galvo, M. Graham, G. Jones, C. Perez von Thun, M. Porkolab, L. Ruchko, D. Testa, P. Woskov, M.A. Albarracin-Manrique, and JET Contributors. The upgraded jet toroidal alfvn eigenmode diagnostic system. *Nuclear Fusion*, 56(11):112020, 2016.

[31] G.T.A. HUYSMANS, J.P. GOEDBLOED, and W. KERNER. Isoparametric bicubic hermite elements for solution of the grad-shafranov equation. *International Journal of Modern Physics C*, 02(01):371–376, 1991.

[32] A. B. Mikhailovskii, G. T. A. Huysmans, S. E. Sharapov, and W. Kerner. Optimization of computational mhd normal-mode analysis for tokamaks. *Plasma Phys. Rep.*, 23:844, 1997.

[33] J. Hedin, T. Hellsten, L.-G. Eriksson, and T. Johnson. The influence of finite drift orbit width on icrf heating in toroidal plasmas. *Nuclear Fusion*, 42(5):527, 2002.

[34] M Jucker, J P Graves, W A Cooper, and T Johnson. Ion cyclotron resonance heating with consistent finite orbit widths and anisotropic equilibria. *Plasma Physics and Controlled Fusion*, 53(5):054010, 2011.

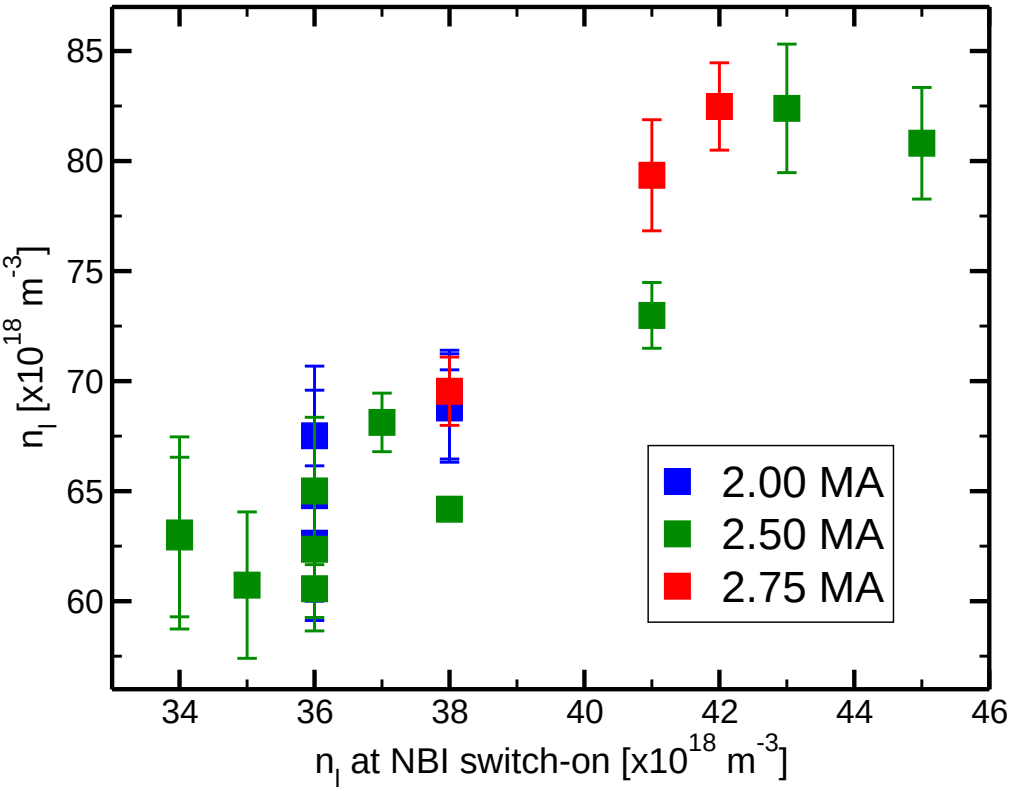

Figure 1. Density at high performance time versus density at NBI switch-on time.

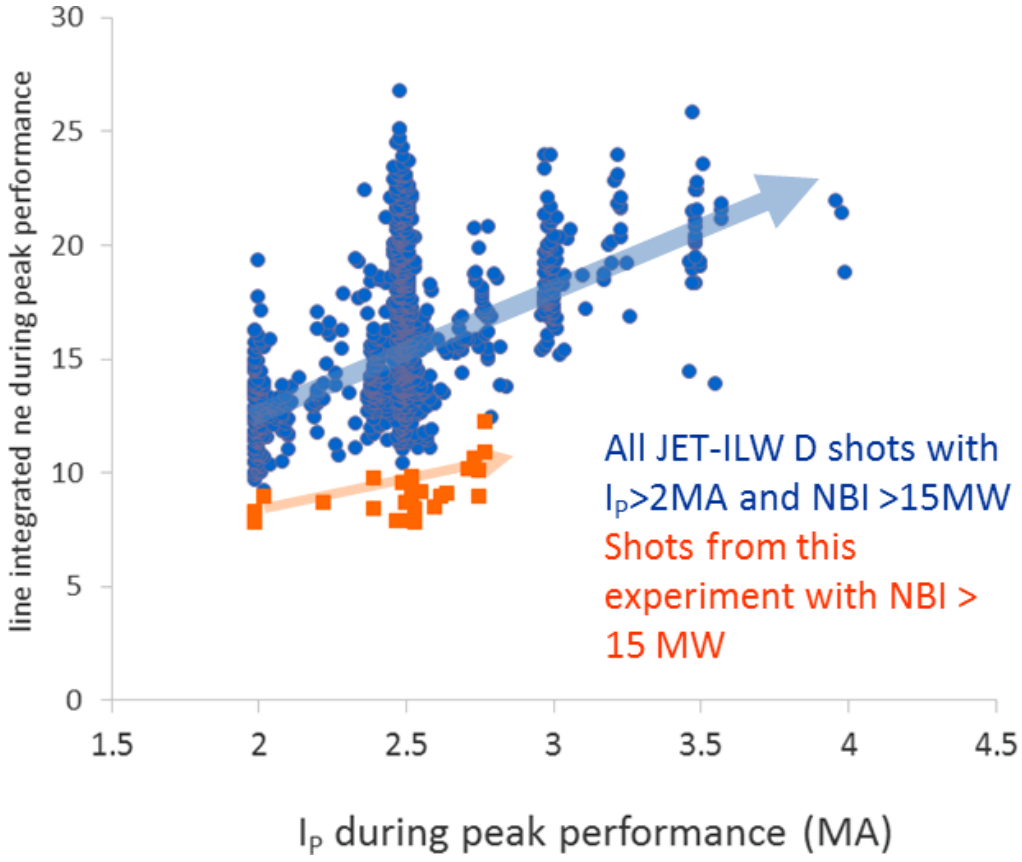

Figure 2. Density versus current at peak performance since the installation of the ITER-like wall in JET. The discharges discussed in this article appear as red symbols.

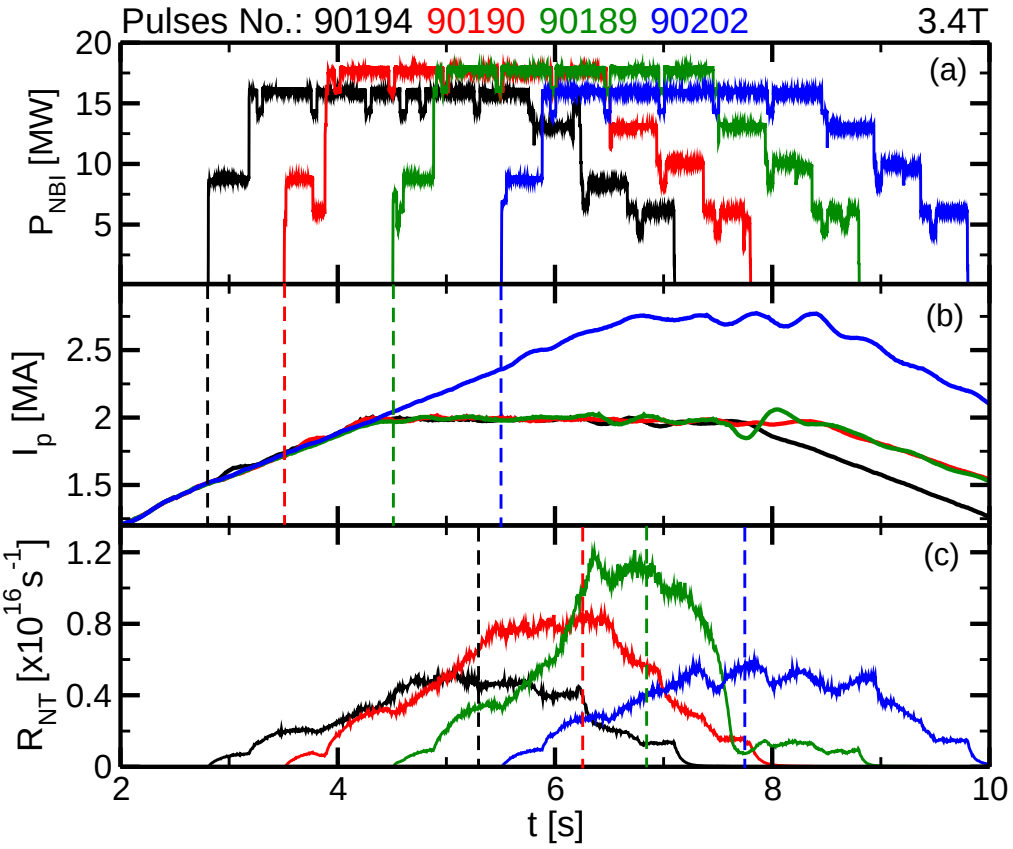

Figure 3. Comparison of pulses #90194, #90190,#90189, #90202, which differ by the time at which the NBI power is applied. (a) NBI power; (b) plasma current; (c) neutron rate. On (a) and (b), the vertical dashed lines show the NBI switch-on time. On (c), the vertical dashed lines show the approximate time of peak performance and refer to Fig. 4.

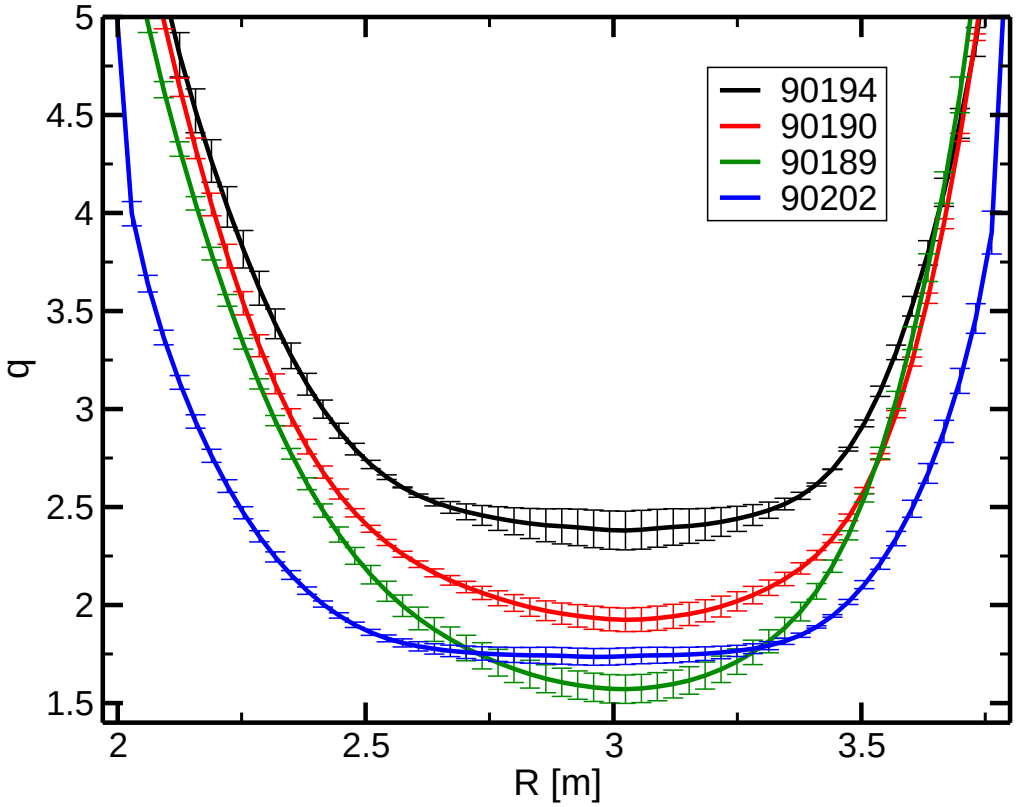

Figure 4. Safety factor profile at peak performance time for #90194, #90190,#90189, #90202 (see Fig. 3).

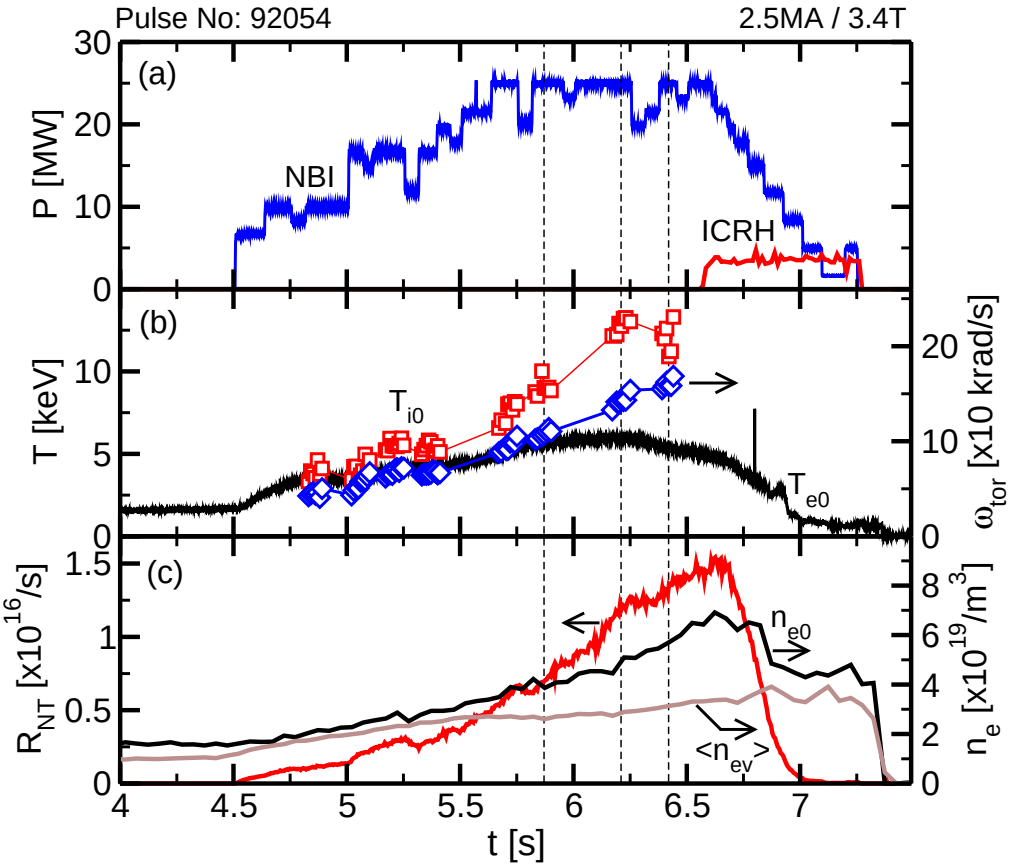

Figure 5. Pulse #92054. (a) Auxiliary power; (b) Central electron and ion temperatures (left y-axis) and toroidal angular pulsation (right y-axis); (c) Neutron rate (left y-axis); central and volume-averaged electron density (right y-axis). The vertical dashed line refer to the profiles shown in Fig. 6.

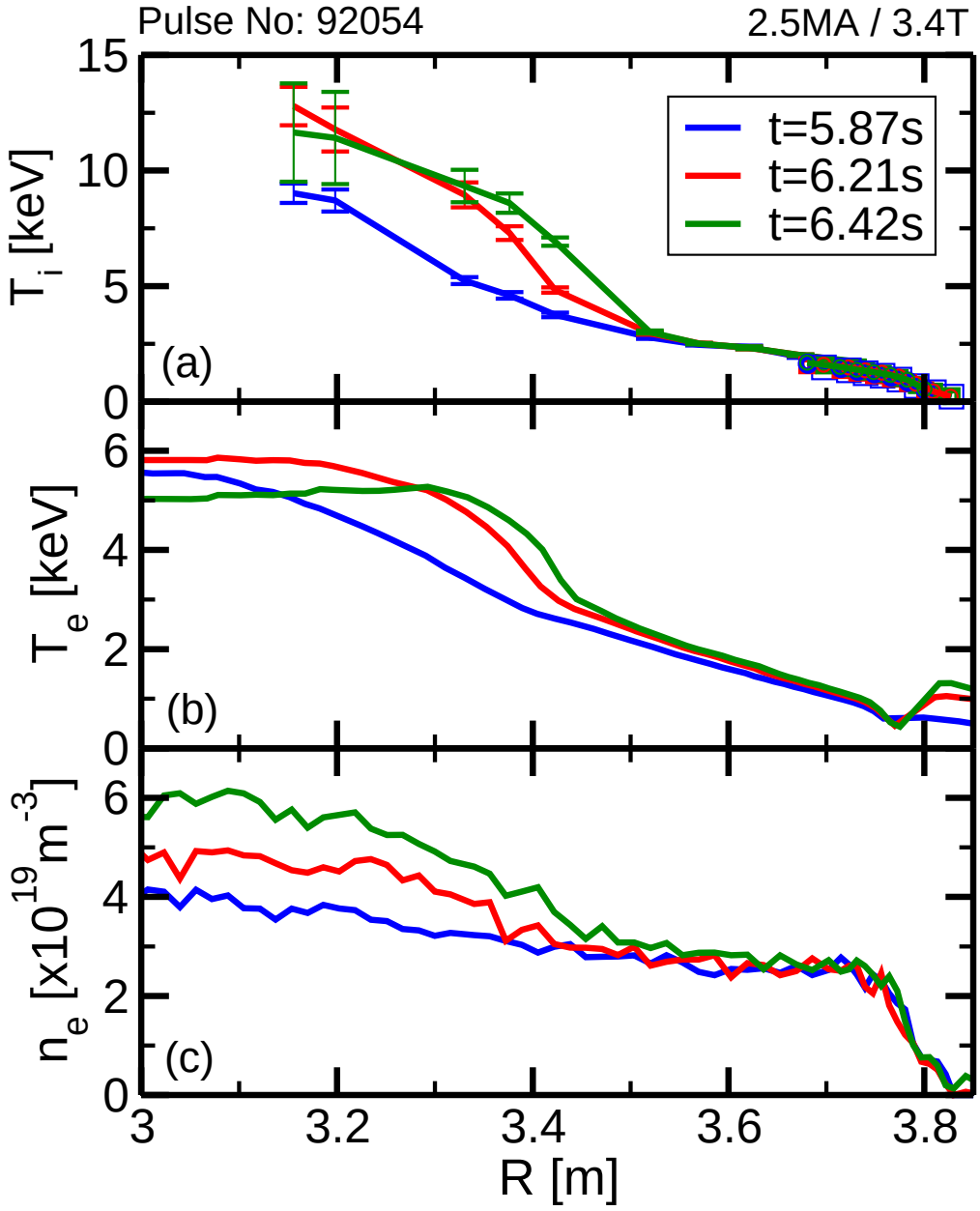

Figure 6. Pulse #92054. (a) Ion temperature from core CXRS (lines and error-bars) and edge CXRS (symbols) diagnostics; (b) Electron temperature from ECE radiometer; (c) Electron density from HRTS system.

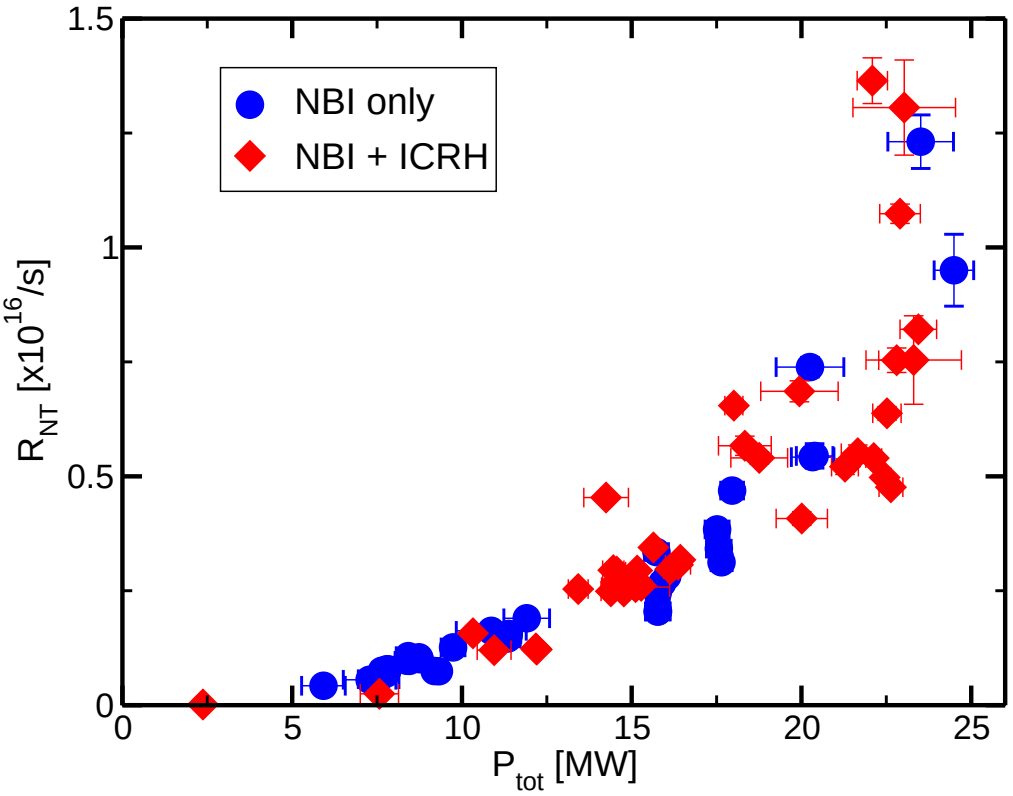

Figure 7. Neutron rate versus total (NBI+RF) power during high-performance phase, including NBI only (squares) and NBI+ICRH (diamonds) phases.

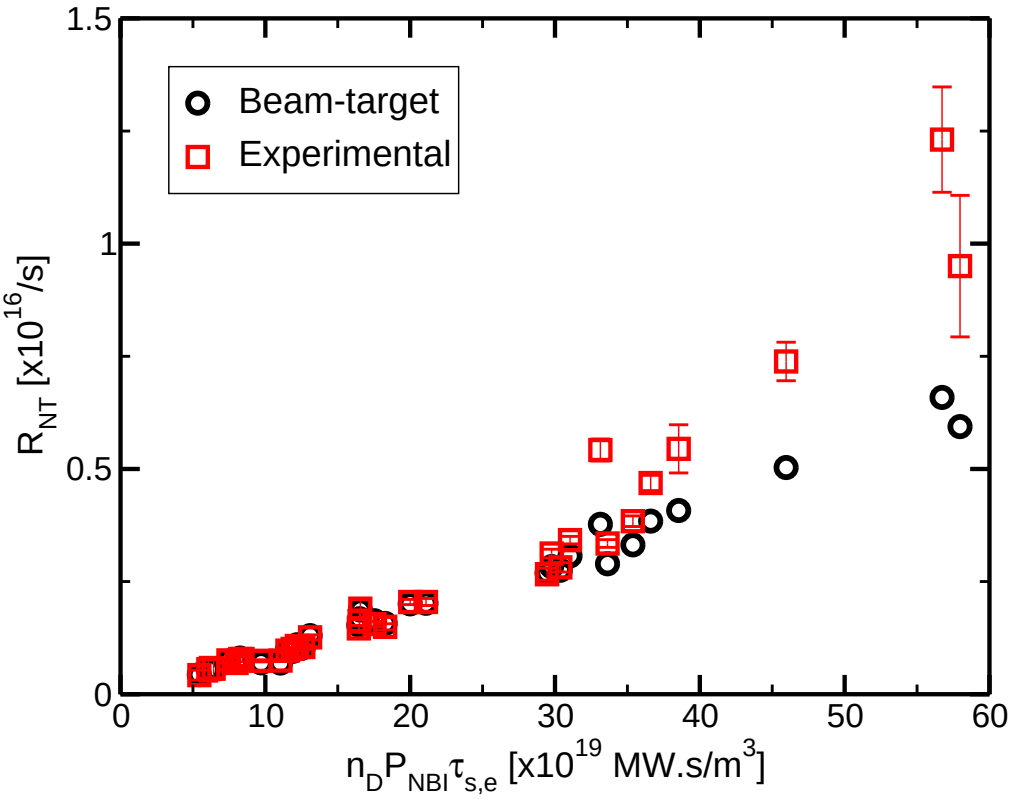

Figure 8. Measured neutron rate (squares) and beam-target neutron rate from PENCIL (circles) versus $n_D P_{NBI} \tau_{s,e}$ at time of peak performance (NBI only pulses).

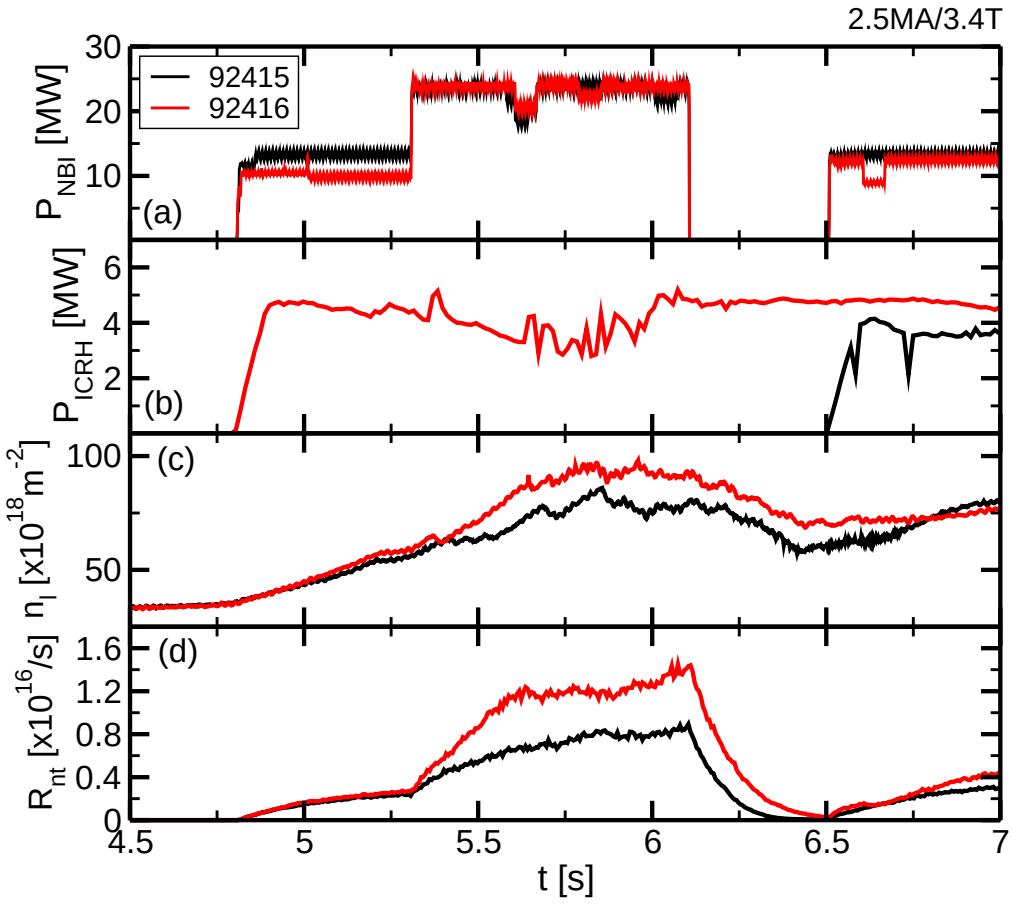

Figure 9. Comparison between pulses #92415 and #92416. (a) NBI power; (b) ICRH power; (c) Line-integrated density; (d) Neutron rate.

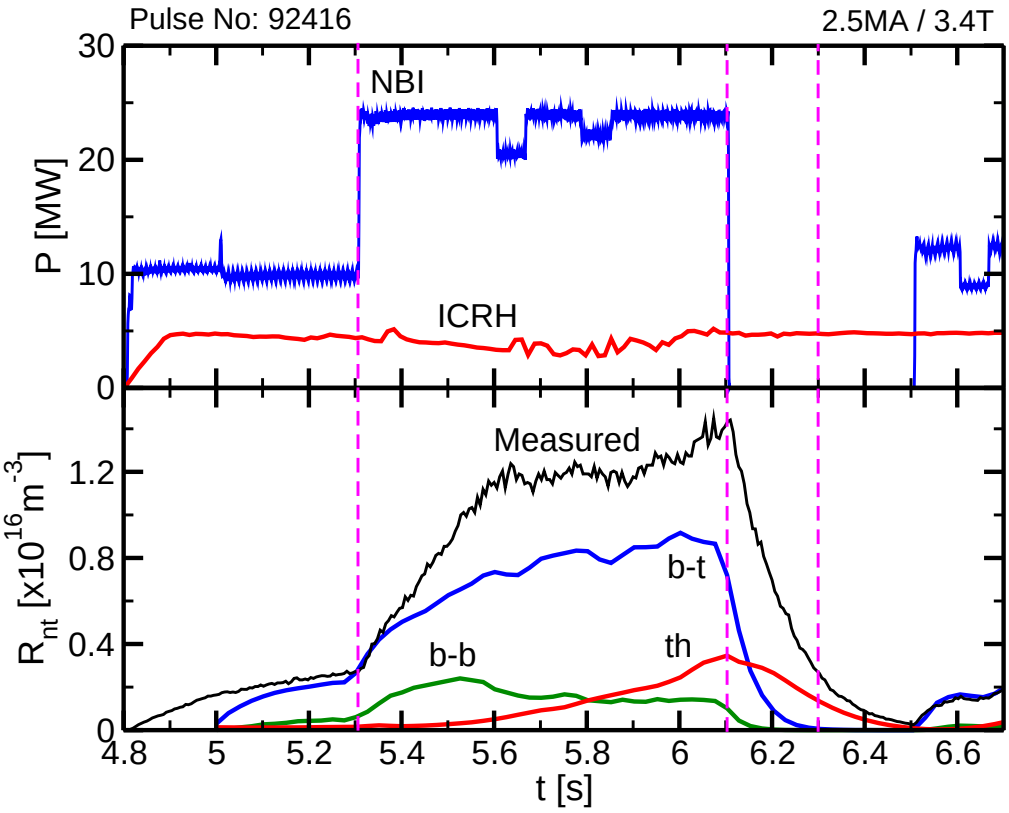

Figure 10. Pulse #92416. (a) NBI and ICRH power; (b) Neutron rate, measured (black line); beam-beam (b-b), beam-thermal (b-t) and thermonuclear (th) contributions computed by TRANSP.

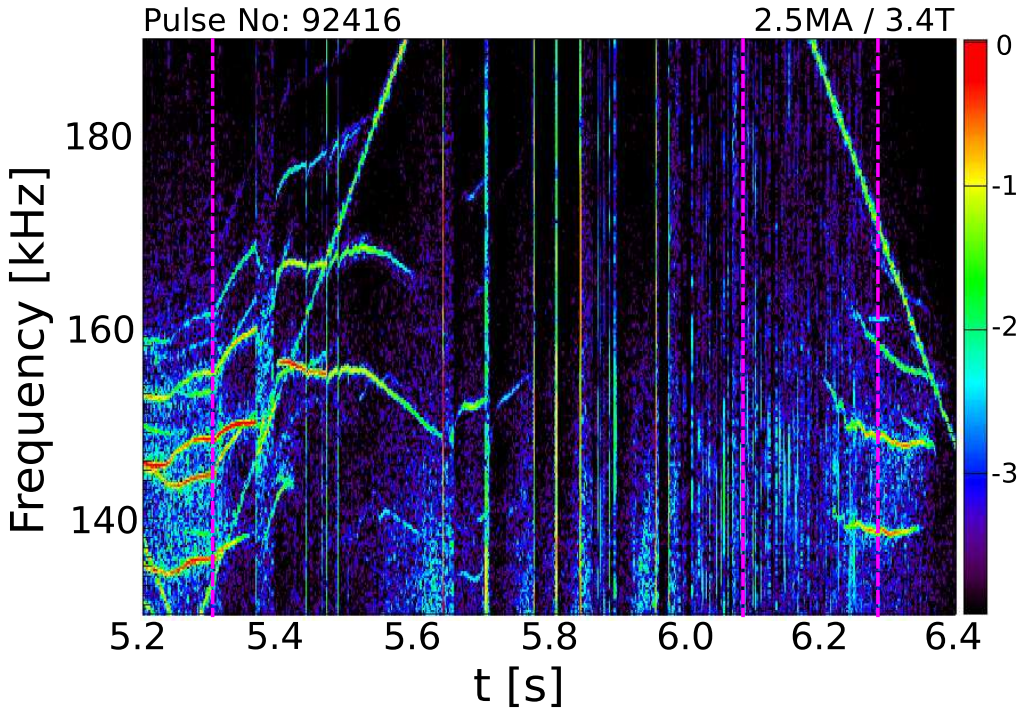

Figure 11. Pulse #92416. Spectrogram from Mirnov coils. The vertical dashed lines refer to Fig. 10.

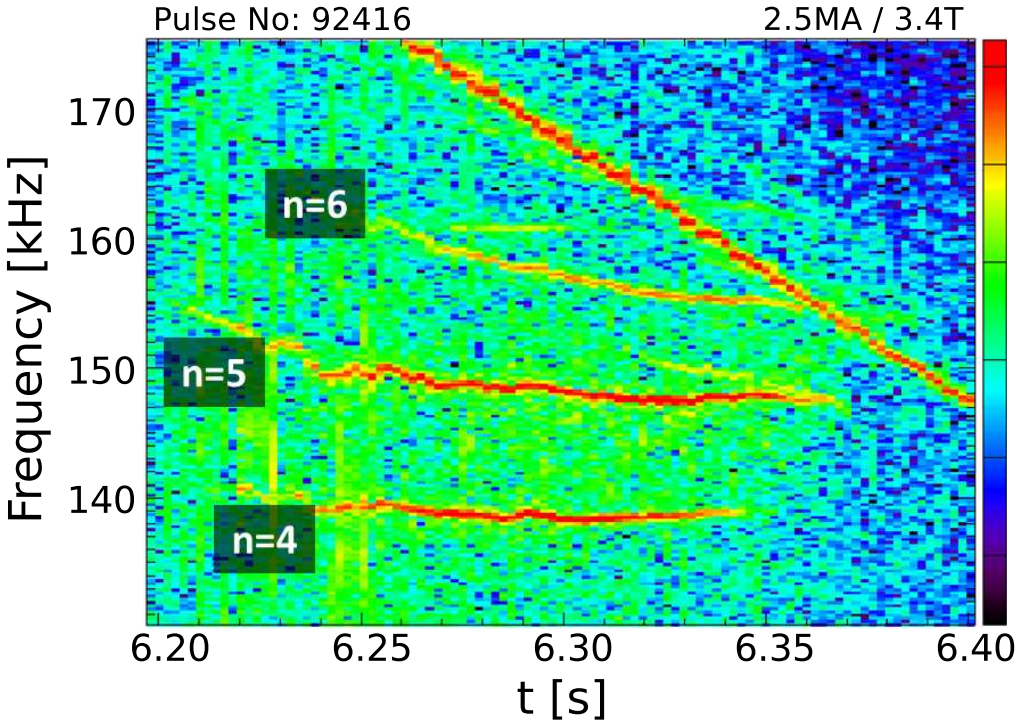

Figure 12. Pulse #92416. TAEs between time 6.20s and 6.40s corresponding to toroidal mode numbers $n = 4, 5$ and 6. The diagonal line on the upper right part of this graph is the TAE antenna signal picked up by the Mirnov coils.

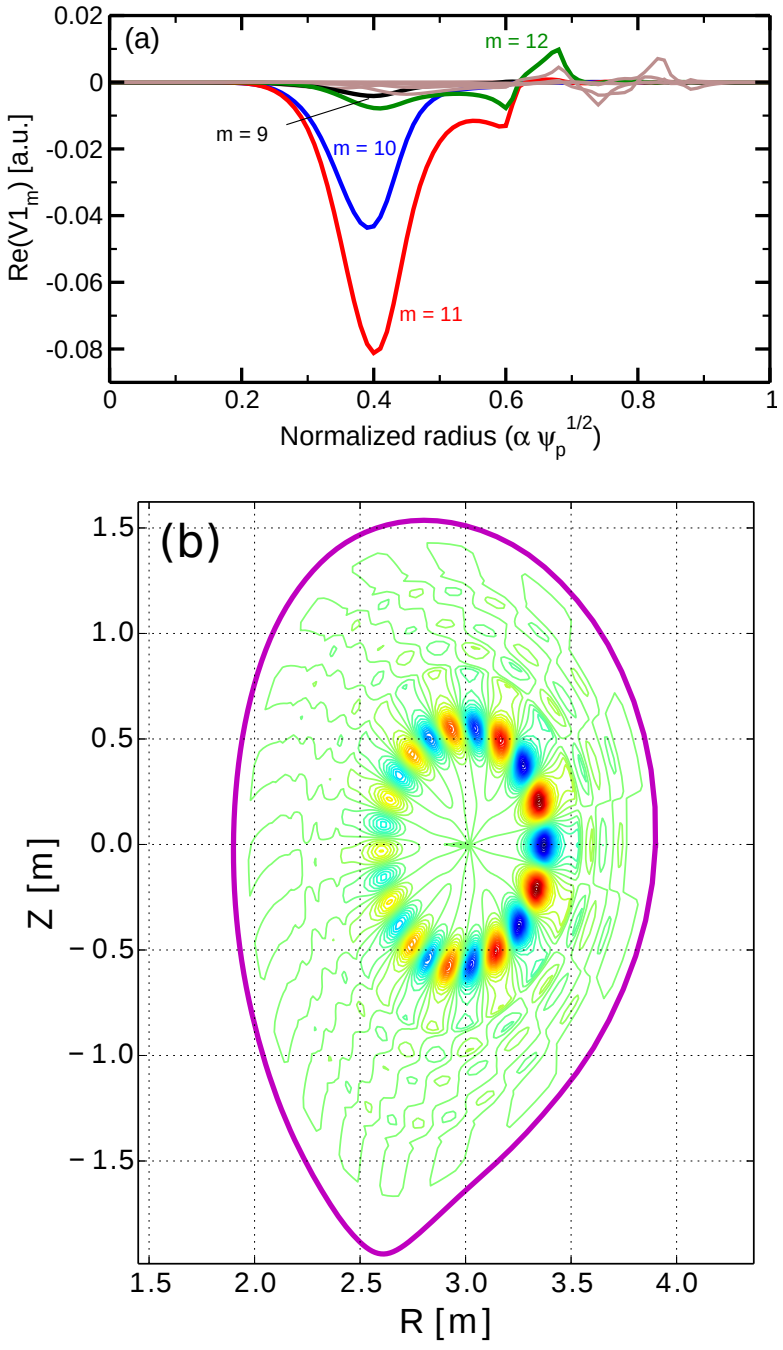

Figure 13. Pulse #92416, MISHKA calculation corresponding to the $n = 5$ TAE shown in Fig. 12 at $t = 6.2s$. (a) Poloidal harmonics; (b) Field reconstruction.

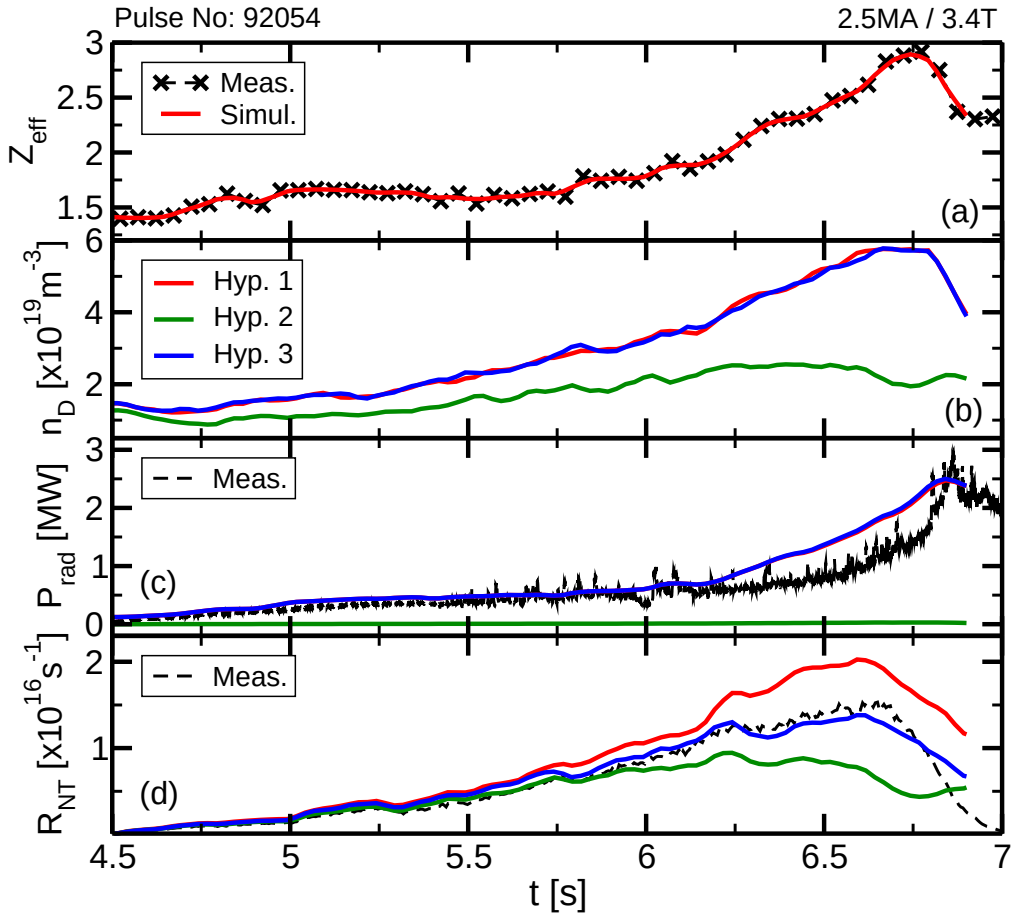

Figure 14. Pulse #92054 interpretative simulation. (a) Effective charge: measured (symbols), used in TRANSP (solid line); (b) Computed deuterium density; (c) Radiative power: measured (dashed line), computed (solid lines); Neutron rate: measured (dashed line), computed (solid lines).

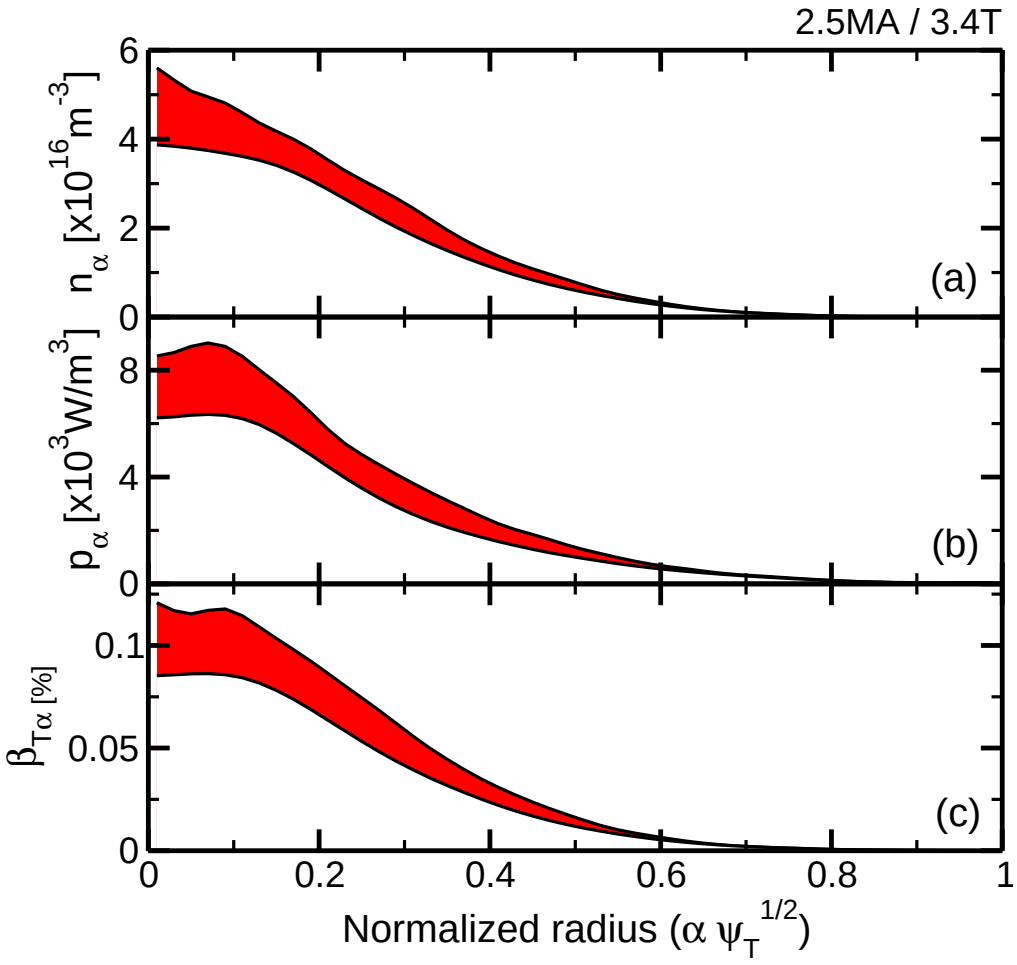

Figure 15. Extrapolation of pulse #92054 to DT. (a) Fusion alpha density; (b) power source from fusion alphas to bulk plasma particles; (c) normalised fusion alpha beta (toroidal). The shaded area is delimited by scenarios 1 and 3 in Fig. 14.